applied sciences

MDPI

Article

Study of the Precipitation Process in Aging Steel Pipeline Weldments by Thermoelectric Power Means

Sergio Ramirez [1], Hector Carreon [1,*], Maria G. Carreon [2], Melchor Salazar [3], Luis Bejar [1] and Ariosto Medina [1]

[1] Instituto de Investigaciones Metalurgicas (UMSNH), Ciudad Universitaria, Morelia 58000-888, Mexico; sergio_unk@hotmail.com (S.R.); lbgomez@umich.mx (L.B.); ariosto@umich.mx (A.M.)
[2] Instituto de Investigaciones Quimico-Biologicas (UMSNH), Ciudad Universitaria, Morelia 58000-888, Mexico; mgcarreon3012@gmail.com
[3] Clúster Politécnico Veracruz (IPN), Veracruz 93400, Mexico; melchor_mtz@yahoo.com
* Correspondence: hcarreon@umich.mx; Tel.: +1-52-443-3167414

Received: 14 August 2018; Accepted: 27 August 2018; Published: 29 August 2018

check for updates

Abstract: The microstructural changes due to the aging process in steel pipeline weldments as a function of the thermoelectric power (TEP) were studied. In general, the thermoelectric methods are based on the well-known Seebeck effect. The thermoelectric methods monitor the TEP via an electron flux induced by a temperature gradient in metallic materials, which is affected by the different types of defects that are present in the atomic lattice, such as atoms in the solid solution, precipitates and dislocations. In this present study, the relationship among the TEP data, hardness and the microstructure of steel pipeline weldments was investigated. In addition, the coarse and dendritic grain structure of the welding material is extremely and unpredictably anisotropic. Such microstructures are no longer direction-independent to the electron flux. Therefore, it has an opposite negative effect on the TEP and overlaps the precipitation effect due to the aging process. TEP and hardness measurements were obtained in each zone of the weldments. For each section of the weldment, the weld bead (WB), heat affected zone (HAZ) and base metal (BM) were found to correspond to particular values of TEP. The relationship between the TEP and the microstructure of a weldment of X60 and X65 micro-alloyed steel that was artificially aged was obtained using the conventional contact TEP technique (hot-tip) and scanning electron microscopy (SEM). It was found that thermoelectric power is very sensitive to the aging process in the two-studied steel pipeline weldments.

Keywords: thermoelectric power; hardness; aging; pipeline; weldment

1. Introduction

Steel pipelines with low carbon contents, welded by an electric arc, have been used for many years in the oil industry. However, the failures that are found frequently during its operation over many years have prompted several studies to study the design, construction, operation and maintenance of equipment and metallic structures that are used in this industry. In general, the steel pipes undergo a natural aging process that is accelerated due to prolonged exposure at operating temperatures (between 25 and 70 °C) and variations in the operating pressure. These operating conditions can cause changes in the microstructure, mechanical properties (elastic limit, hardness, ductility and toughness), type of fracture and probability of failure after several years of service. This natural aging process is described by two factors: the peak of aging associated with the maximum resistance and precipitation of carbides that interact with the dislocations and causes hardening by precipitation; and the over-aging related to the decrease in resistance and thickening of carbides after a long aging time [1,2].

On the other hand, the thermoelectric power (TEP) is a valued intrinsic material property, which depends on microstructural features. Since the micro-alloyed steel microstructure correlates directly to the material properties, TEP provides an effective way to characterize the microstructural changes, which can potentially lead to significant localized imperfections and possible structural failures in a time-dependent phase transformation (including aging). It is also well known that TEP is a function of electronic scattering behavior, electron concentration and effective mass of the electrons in a metallic alloy. These physical factors are influenced by the material microstructural and phase transformation changes. In this present study, the relationship between the TEP and the microstructure was obtained using the conventional contact TEP technique (hot-tip) and SEM for weldments of X60 and X65 micro-alloyed steel that are artificially aged.

2. Thermoelectric Technique

The thermoelectric methods are based on the Seebeck effect, which is commonly used in thermocouples to measure temperatures. Figure 1 shows the schematic diagram of the hot tip thermoelectric measurement as most are often performed for the characterization of materials. One of the reference electrodes is heated by electrical means to a preset temperature (T_h), which acts essentially as the tip of a temperature-stabilized soldering iron, while the other electrode is left to be 'cold' at room temperature (T_c). The measurement is obtained quickly in a few seconds to ensure that the hot reference electrode is not noticeably cooled down by the specimen and that the rest of the specimen beyond the close vicinity of the contact point is not perceivably warmed up. After this, the measured thermoelectric voltage due to the Seebeck effect is given by:

$$V = \int_{T_c,}^{T_h} [S_S(T) - S_R(T)]dT = \int_{T_c}^{T_h} S_{SR}(T)dT \quad (1)$$

where T is the temperature; and S_S and S_R denote the absolute thermoelectric powers of the specimen and the reference electrode, respectively. Any variation in the material properties can affect the measured thermoelectric voltage via $S_{SR} = S_S - S_R$, which is the relative thermoelectric power of the specimen that is tested with respect to the reference electrode. In most cases, the temperature-dependence of the thermoelectric power can be neglected over the range of operating parameters used and the thermoelectric voltage can be approximated as $V \approx (T_h - T_c)$ S_{SR}. Ideally, regardless of how high the temperature difference between the junctions is, only the thermocouples made of different materials, or more precisely materials of different thermoelectric powers, will generate a thermoelectric signal.

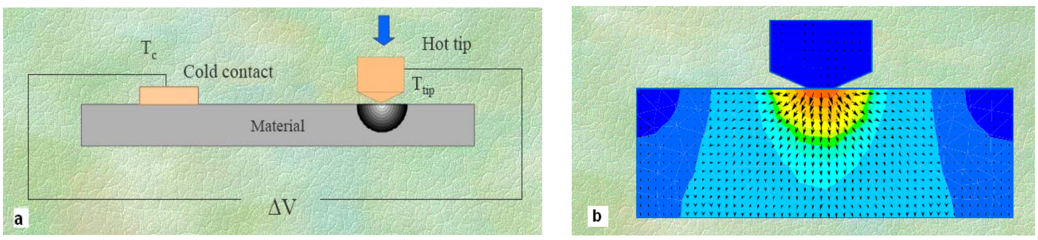

Figure 1. Schematic diagram of the (**a**) hot tip thermoelectric method and the (**b**) thermal gradient inside the sample.

This unique feature makes the simple thermoelectric tester one of the most sensitive material discriminators that are used in nondestructive inspection. Figure 1b shows the thermal gradient produced inside the sample by using the *hot tip method*. Some advantages of the above-described thermoelectric method are: localized TEP measurements and thus, ability to detect heterogeneities; possibilities to measure the 2D TEP map of massive materials; adjustment of the measured zone by changing the tip size; possibility of Non-Destructive Testing (NDT) directly on massive materials (in-situ measurements). The most important parameters affecting the thermoelectric measurements are those associated with volumetric and contact effects. The volumetric effect is closely related to the thermoelectricity phenomena due to the kinetics of the diffusion of electrons throughout the material. This effect is mainly affected by chemical composition, different heat treatment, precipitation process, grain boundaries, texture and fatigue of the material [3–5]. The contact effects are related to the imperfect contact between the test sample and the reference probe/block, amount of pressure applied to the probe/block, temperature of hot and cold junctions and probe/block material.

3. Experimental Method

In this present study, the two weldments of different steel pipelines used in the oil industry, which are namely API X60 and X65, were studied. These micro-alloyed steel pipelines were manufactured by Productora Mexicana de Tuberia (PMT), which have a diameter of 106.68 cm (X60) and 60.96 cm (X65) with a wall thickness of 1.42 cm (X60) and 1.27 cm (X65). The welding process used was Submerged Arc Welding (SAW) in two-passes. The chemical composition of these steels is shown in Table 1. The two materials were subjected to different heat treatments. Firstly, the materials were normalized by holding at 1200 °C for 1 h, which was followed by water cooling/quenching. After this, the two micro-alloyed steels were aged at 300 °C for different aging times that ranged from 1 min to 30 h for the X60 weldment and from 1 min to 45 h for the X65 weldment in order to promote the formation of precipitates.

Table 1. Chemical composition of X-60 and X-65 micro-alloyed steels (wt%).

Steel	C	Mn	Si	P	S	Al	Nb	Cu	Cr	Ni	V	Ti
X60	0.025	1.57	0.14	0.012	0.002	0.044	0.097	0.31	0.29	0.17	0.002	0.014
X65	0.04	1.48	0.25	0.12	0.002	0.041	0.047	0.1	0.02	0.08	0.07	0.017

The characterization of the weldment was conducted through Optical Microscopy (OM) and Scanning Electron Microscopy (SEM). The specimens used in the characterization by the microscopy techniques were etched using 2% Nital and 50%, respectively. The characterization of the inclusions was evaluated by SEM using energy dispersive X-ray spectroscopy (EDS) microanalysis. Hardness measurements were carried out using a Rockwell scale in the metal base (BM), heat affected zone (HAZ) and the weld bead (WB).

The thermoelectric (TEP) measurements were performed using a calibrated ATS-6044T Alloy Thermo-Sorter. This instrument is a thermoelectric alloy tester that is used in NDT, which provides relative readings with arbitrary units. Therefore, this must first be calibrated by materials of known absolute thermoelectric powers [6]. The *hot tip thermoelectric instrument* settles the temperature difference by the means of a dual tipped reference probe. One tip is at room temperature (25 °C) and the other is heated to a specific temperature (50 °C). In our case, an annealing copper hot tip (standard probe) was used in order to measure the thermoelectric power of the weldments of X60 and X65 micro-alloyed steel artificially aged samples. The dual-tipped probe was placed on the three main zones (BM, HAZ and WB) of the weldments, before an electric circuit was completed to generate a signal. This signal was then processed to obtain a peak-to-peak reading, which is displayed on the microvolts digital display. The reading is representative of the crystalline microstructure changes in the material.

4. Results and Discussion

Knowledge of the weldment microstructure is essential for understanding the TEP data. Figure 2a,b and Figure 3a,b clearly show the different microstructures obtained in the API X60 and X65 micro-alloyed weldments. We clearly observed a columnar structure of welding metal in the outer portion of the weldment. Furthermore, we also found a reheat affected zone (RHAZ) between the two weld beads. The HAZ from the first weld bead (WB 1) is affected by the HAZ of the second weld bead (WB 2), producing a microstructure with a smaller grain size. Furthermore, the fusion zone (FZ) was also observed. Figures 2c and 3c show that the HAZ of the weld bead is mainly made up by polygonal and coarse acicular ferrite. This microstructure optimizes the strength and toughness in the weld beads. Finally, Figures 2d and 3d show the microstructure of the BM in API X60 and API X65 steel, which consists of polygonal ferrite (light areas) and pearlite (dark areas).

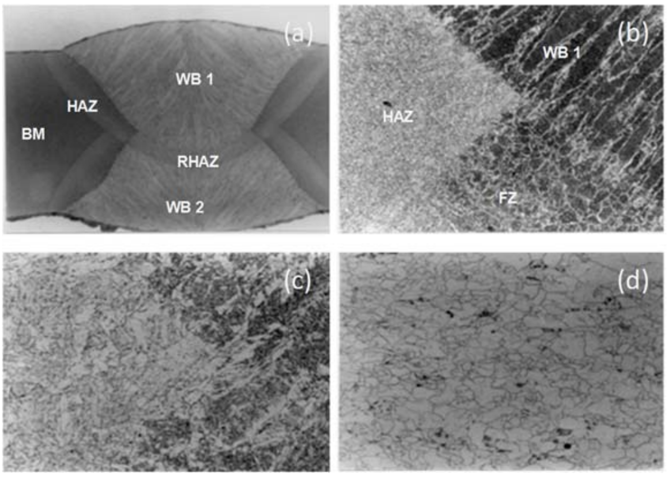

Figure 2. Microstructures of API X60 micro-alloyed steel weldment: (**a**) Weldment zones; (**b**) Microstructure showing the FZ, HAZ and WB 1; (**c**) interface between HAZ and WB; and (**d**) Base Metal (BM), ferrite (light areas) and pearlite (dark areas).

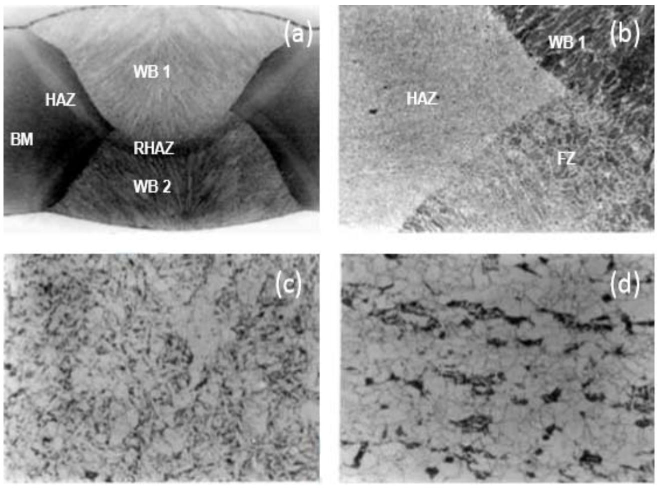

Figure 3. Microstructures of API X65 micro-alloyed steel weldment: (**a**) Weldment zones; (**b**) Microstructure showing the FZ, HAZ and WB 1; (**c**) interface between HAZ and WB; and (**d**) Base Metal (BM), ferrite (light areas) and pearlite (dark areas).

In the X-65 steel (Figure 3d), there is a greater quantity of pearlite. The weldments are the main examples of structural components where the final mechanical properties depend on the features of the microstructure obtained after the welding process [7].

On the other hand, the SEM analysis performed on the aged samples revealed the thin dispersed precipitation of particles that were trans-granular, semi-round and fine (100–900 nm). Furthermore, these participles contained Fe-C as detected by EDS microanalysis. These nanoprecipitates showed preferential nucleation and interactions with the dislocations in ferritic grains, which is shown in

Figures 4b–d and 5b–d. Fine Fe_3C and Fe_2C precipitates that are 50–200 nm in size are homogeneously distributed in the ferritic grains of the API X-65 and API X-65 micro-alloyed steels after different aging times. The precipitation of these particles induces the hardening of the weld joint. The dispersion of fine particles with heterogeneous nucleation and precipitation in the dislocations of the surroundings causes more obstacles and strong interactions. This blocks and delays the movement of the dislocations, resulting in an increase in mechanical properties, such as resistance. The quantitative analysis of this increase in the density of nanoparticles is represented as a function of aging time.

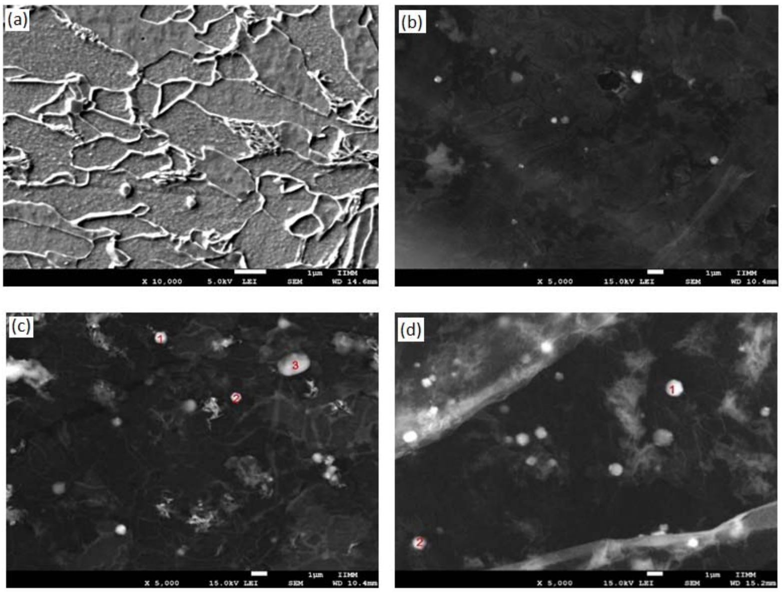

Figure 4. SEM micrographs of the (**a**) API-X60 weldment that was over-aged at 300 °C for three different aging times of (**b**) 6 h, (**c**) 15 h and (**d**) 30 h, respectively, showing fine Fe_3C and Fe_2C precipitates that were homogeneously distributed in ferritic grains.

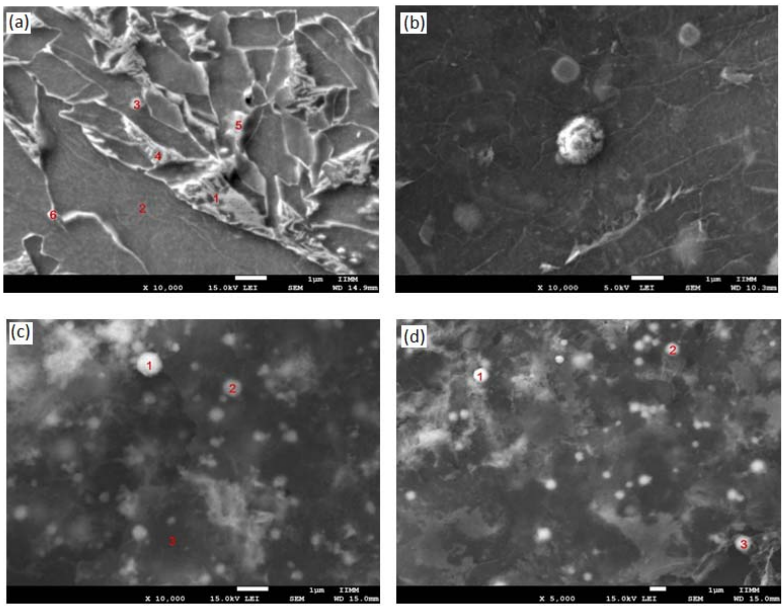

Figure 5. SEM micrographs of the (**a**) API-X65 weldment that was over-aged at 300 °C for three different aging times of (**b**) 6 h, (**c**) 15 h and (**d**) 45 h, respectively, showing fine Fe_3C and Fe_2C precipitates that were homogeneously distributed in ferritic grains.

The Vickers microhardness values for the API-5L X-60 and X-65 steels (see Figure 6a,b, respectively) show a tendency to increase in the early aging times at the three different zones of the weldment. This phenomenon is attributed to the precipitation of cementite (Fe_3C) and the precipitation of carbide-ε (Fe_2C). The precipitation of carbides occurs mainly in the dislocations within the grain, resulting in the increase in hardness. After this, a considerable decrease in hardness can be observed due to the thickening of the cementite at the expense of the precipitates of smaller cementite and the carbide-ε. The obtained values of hardness are inside of the limits that are recommended for avoiding fractures and cracking in the weldment.

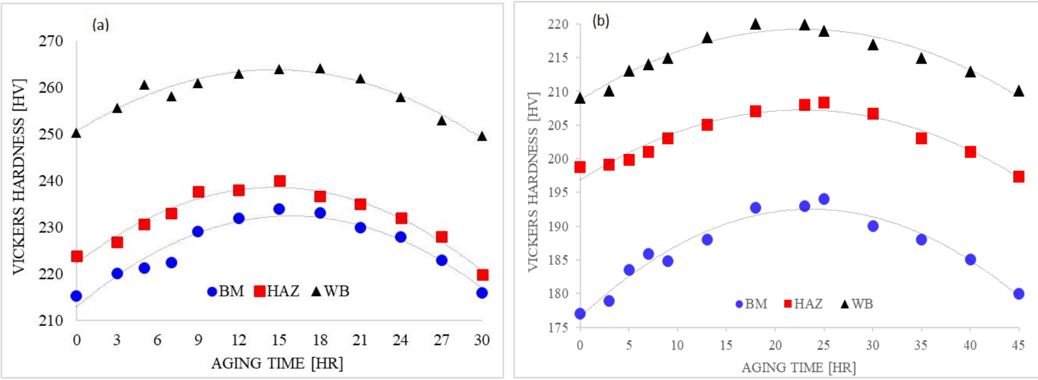

Figure 6. Hardness measurements in the weldments of (**a**) API X60 and (**b**) API X65.

Figure 7 shows the time evolution of the TEP signal for the two micro-alloyed pipeline steels with three different microstructure welding zones at several aging temperatures, which were regularly measured by the contact TEP technique. For all aging temperatures, there is a drop in the TEP values up to around 10 h, before the TEP increases. This is observed in both micro-alloyed artificially aged X60 (Figure 7a) and X65 (Figure 7b) steels, respectively. Therefore, the relationship between the microstructure and TEP will be addressed in more detail in the following sections.

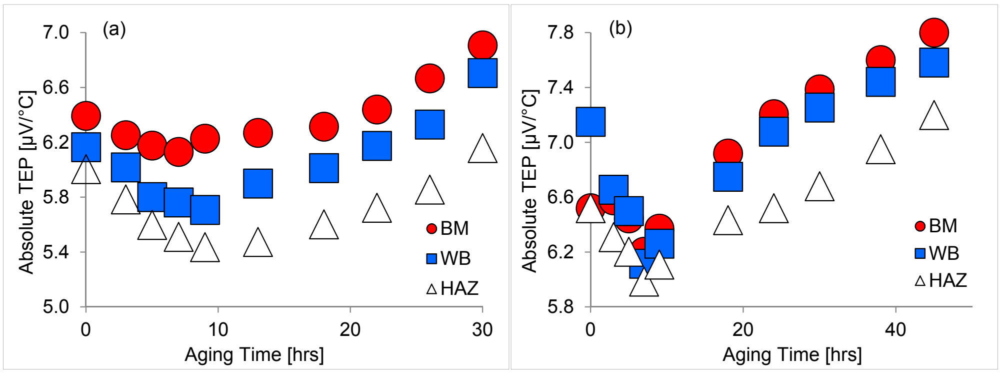

Figure 7. Thermoelectric power measurements of the micro-alloyed steel of (**a**) API X60 and (**b**) API X65 weldments that were artificially aged.

At this point, it can be concluded that in the first stage of the aging process, the depletion or enrichment of the matrix from the precipitating elements and the noticeable microstructural changes in the three main welded zones are the main factors that influenced the decrease in the TEP values. An equiaxed grain was present in the base metal (BM). In the weld bead (WB), an elongated grain was observed. Finally, at the heat affected zone (HAZ), a mixture of equiaxed and elongated grains developed. In our case, the initial TEP decrease seems to be related to the inhomogeneity of the grain size/shape, which induces anisotropy in the medium. This anisotropy has an opposite negative effect on the TEP and overlaps the precipitation effect due to the aging process induced by the heat treatments.

In the second stage of the aging process, the precipitation of the particles (Fe_3C) and carbide-ε (Fe_2C) is very pronounced, which is shown in Figures 4 and 5. The volume fraction increases, which has a positive effect on the TEP. In addition, the precipitates are likely to have an intrinsic effect on the TEP [8]. In the case of metallic alloys [6,9–13], it was clearly shown that the coarse incoherent precipitates have no effect on the TEP, while the coherent and semi-coherent precipitates have a strong influence. These results can be easily explained by the fact that the incoherent precipitates do not induce internal stresses in the matrix that are likely to disturb the lattice and thus, act like voids in the matrix with little influence on the TEP. In contrast, the coherent and semi-coherent precipitates induce elastic stresses in the lattice and thus, modify the TEP. It was observed that this modification depends on the size, nature, morphology and volume fraction of the precipitates. The microstructural changes due to the aging process in the micro-alloyed steel as a function of the TEP measurements should be further studied.

5. Conclusions

The precipitation behavior in the weldments of API X60 and API X65 micro-alloyed steels has been studied using thermoelectric power and hardness measurements. The study clearly revealed that the most important microstructural parameters that are likely to affect the electron flux are the precipitation process and their grain size/shape. It has been shown that the major cause of the initial decrease in TEP in the first stage of the aging process is the depletion or enrichment of the matrix from the precipitating elements and the anisotropy due to the presence of different microstructures at the main welded zones. Finally, the increase in TEP after a long aging time is attributed to the precipitation of the nanoparticles (Fe_3C) and carbide-ε (Fe_2C), although further studies examining this are required. It is concluded that the thermoelectric power technique is very sensitive to microstructural changes and it can be used reliably for the evaluation or monitoring of precipitates in the aging processes of steel weldments.

Author Contributions: Methodology, H.C., S.R., M.G.C., M.S., L.B., A.M.; Investigation, H.C., S.R., M.G.C., M.S., L.B., A.M.; Writing-Review & Editing, H.C., M.G.C.; Supervision, H.C.; Project Administration, H.C.

Funding: This research received no external funding.

Acknowledgments: This work was performed at UMSNH-MEXICO with partially funding from CONACYT-MEXICO under project CB-2015/256013 and Prodep/CA-140.

Conflicts of Interest: The authors declare no conflict of interest.

Nomenclature

V	thermoelectric voltage
T	temperature
T_h	preset temperature
T_c	room temperature
S_S	absolute thermoelectric powers of the specimen
S_R	absolute thermoelectric powers of the reference electrode
SEM	Scanning Electron Microscopy
TEP	Thermoelectric Power
API	American Petroleum Institute
EDS	Energy Dispersive Spectroscopy
BM	Base Metal
HAZ	Heat Affected Zone
RHAZ	Reheat Affected Zone
FZ	Fusion Zone
WB	Weld Bead

WB 1	First Weld Bead
WB 2	Second Weld Bead
SAW	Submerged Arc Welding
wt%	percent by weight
NDT	Non-Destructive Testing

References

1. Greer, J.B. Factors affecting the stress cracking performance of high strength steel. *Mater. Perform.* **1975**, *14*, 11–21.
2. Craig, B.D. Calculating the lowest failure pressure for electric resistance welded pipe. *Weld. J.* **1998**, *40*, 61–63.
3. Caballero, F.G.; Capdevila, C.; Alvarez, L.F.; García de Andrés, C. Thermoelectric power studies on a martensitic stainless steel. *Scr. Mater.* **2004**, *50*, 1061–1066. [CrossRef]
4. Carreon, H.; Barriuso, S.; Lieblich, M.; González-Carrasco, J.L.; Jimenez, J.A.; Caballero, F.G. Significance of the contacting and no contacting thermoelectric power measurements applied to grit blasted medical Ti6Al4V. *Mater. Sci. Eng. C* **2013**, *33*, 1417–1422. [CrossRef] [PubMed]
5. Kawaguchi, Y.; Yamanaka, S. Applications of thermoelectric power measurement to deterioration diagnosis of nuclear material and its principle. *J. Nondestruct. Eval.* **2004**, *23*, 65–76. [CrossRef]
6. Barnard, R.D. *Thermoelectricity in Metals and Alloys*; Taylor and Francis: Abingdon, UK, 1972.
7. Carreón, H.; Barrera, G.; Natividad, C.; Salazar, M.; Contreras, A. Relation between hardness and ultrasonic velocity on pipeline steel welded joints. *Nondestruct. Test. Eval.* **2016**, *31*, 97–108. [CrossRef]
8. Carreon, H.; San Martin, D.; Caballero, F.G.; Panin, V.E. The effect of thermal aging on the strength and the thermoelectric power of the Ti-6AL-4V alloy. *Phys. Mesomech.* **2017**, *20*, 447–456. [CrossRef]
9. Kleber, X. Detection of surface and subsurface heterogeneities by the hot tip thermoelectric power method. *NDT E Int.* **2008**, *41*, 364–370. [CrossRef]
10. Mott, N.F.; Jones, H. *The Theory of the Properties of Metals and Alloys*; Dover Publications: Mineola, NY, USA, 1958.
11. Kawaguchi, Y.; Yamanaka, S. Mechanism of the change in thermoelectric power of cast duplex stainless steel due to thermal aging. *J. Alloys Compd.* **2002**, *336*, 301–314. [CrossRef]
12. Coste, J.F.; Leborgne, J.M.; Massoud, J.P.; Grisot, O.; Miloudi, S.; Borrelly, R. Application of Thermoelectricity to NDE of Thermally Aged Cast Duplex Stainless Steels and Neutron Irradiated Ferritic Steels. In Proceedings of the EPRI Workshop on NDE for Damage Assessment, La Jolla, CA, USA, 6–7 October 1997.
13. Grisot, O.; Massoud, J.P. Evaluation of the Thermal Ageing of Duplex Stainless Steels. In Proceedings of the International Conference on Nuclear Engineering, 26–30 May 1997.

© 2018 by the authors. Licensee MDPI, Basel, Switzerland. This article is an open access article distributed under the terms and conditions of the Creative Commons Attribution (CC BY) license (http://creativecommons.org/licenses/by/4.0/).